

Fatigue damage accumulation in a structural steel (42CrMo4) subjected to axial/torsional bi-axial loadings

M. de Freitas, L. Reis and B. Li

Department of Mechanical Engineering, Instituto Superior Técnico
Av. Rovisco Pais, 1049-001 Lisboa, Portugal
E-mail: mfreitas@dem.ist.utl.pt, luís.g.reis@ist.utl.pt, bli@ist.utl.pt

ABSTRACT. *Fatigue damage accumulation is a paramount issue in estimation fatigue life of a component or structure. The objective of present paper is to understand the mechanism of fatigue damage accumulations subjected to multiaxial loading, focus is on the studies of the effect of sequence and asynchronous biaxial load history to damage accumulation. Both experimental and numerical methods are applied to study the cyclic deformation behaviour, crack initiation and crack path orientation. A structural steel is studied (42CrMo4) and various biaxial loading paths were applied in experimental tests to observe the effects of multiaxial loading paths on fatigue life and crack initiation/orientation. Fractographic analyses of the plane orientations of crack initiation and propagation were carried out by optical microscope and SEM approaches. It is observed the effects of loading sequence and asynchronous on the fatigue life, crack orientation and fracture morphology. The advanced plasticity model of Jiang and Sehitoglu is applied for evaluating the cyclic stress/strain. Theoretical estimations of the damage plane are conducted using some critical plane approaches and compared with experimental results. Based on achieved results damage accumulation process is discussed and some remarks are drawn.*

INTRODUCTION

Many engineering components and structures are exposed to complex and combined service load sequences that cause local multiaxial stress states at the critical material element. To increase the accuracy of fatigue life estimation, it is very important to understand the mechanism of damage accumulations subjected to service multiaxial loading histories. In the literature several fatigue damage accumulation models have been proposed for uniaxial loading cases as reviewed by Fatemi and Yang [1], however, relatively very little attention had been paid for multiaxial loading cases. Weiss and Pineau [2] studied the continuous and sequential multiaxial low-cycle fatigue damage in 316 stainless steel, the sequential tests included two independent successive phases, with different types of loading. During the first phase a variable percentage of fatigue life is applied with a given loading mode (for example, push/pull), followed by another type of loading (for example, fully reversed torsion) applied to failure. Both optical and scanning electron microscopy (SEM) were used to analyse the failure modes, the

orientation of microcracks and macrocracks, and crack densities. It was concluded that at room temperature, sequential torsion – tension/compression tests lead to fatigue lives much lower than those calculated using the Miner linear damage rule, while sequential tension/compression – torsion tests are much less damaging.

Ott et al [3] proposed an event independent cumulative damage model (EVICD) for the fatigue damage evaluation under general multiaxial stress state and loading conditions. The model takes the plastic strain energy as the major contributor to the fatigue damage. The application of the EVICD model does not require a cycle counting method for general random loading. The previous researches had demonstrated that the cyclic plasticity and loading sequence have significant influences on the fatigue damage accumulation. In the present paper, further studies have been carried out for understanding the mechanism of fatigue damage accumulation subjected to multiaxial loading; focus is on the studies of the effect of sequence of biaxial load history to damage accumulation.

A structural steel is studied, the low alloy steel 42CrMo4. Various biaxial loading paths were applied in the tests to observe the effects of multiaxial loading paths and sequence on the additional hardening, fatigue crack initiation, and crack propagation orientation. Fractographic analyses of the plane orientations of crack initiation and propagation were carried out by optical microscope and SEM approaches.

Numerical simulations were conducted by application of the advanced plasticity model of Jiang and Sehitoglu [4]. In present study, experimental tests were carried out in load control, therefore the cyclic strains were calculated with the cyclic stresses as input to the model. Then, theoretical estimations of the damage plane are conducted using the critical plane approaches. Through both numerical and experimental studies, the effects of loading path and sequence on fatigue damage accumulation and fracture morphology are characterized and compared. It is also shown that the simulated results are in close agreement with experimental observations.

MATERIAL, SPECIMENS AND EXPERIMENTAL PROCEDURE

A structural steel is studied in this work, the high strength quenched and tempered at 525°C steel, 42CrMo4, which microstructure is bainitic. This material was chosen because it is representative of a material regularly used in engineering applications where the risk of failure is highly prevalent and where it will be most valuable to obtain a deeper understanding of its fatigue behaviour. The chemical composition, monotonic and cyclic mechanical properties are shown in Tables 1 and 2, respectively. The geometry and dimensions of the specimens used are shown in Fig. 1.

Table 1. Chemical composition of AISI 303 and 42CrMo4 steels in (wt%)

	C	Si	Mn	P	S	Cr	Ni	Mo	Cu
<i>42CrMo4</i>	0.39	0.17	0.77	0.025	0.020	1.10	0.30	0.16	0.21

Table 2. Monotonic and uniaxial cyclic mechanical properties of the studied materials

<i>42CrMo4</i>		
Tensile strength	σ_u (MPa)	1100
Yield strength	$\sigma_{0.2\%}$ (MPa)	980
Young's modulus	E (GPa)	206
Elongation	A (%)	16
Cyclic Yield strength	$\sigma'_{0.2\%}$ (MPa)	640
Strength coefficient	K' (MPa)	1420
Strain hardening exponent	n'	0.12
Fatigue strength coefficient	σ'_f (MPa)	1154
Fatigue strength exponent	b	-0.061
Fatigue ductility coefficient	ϵ'_f	0.18
Fatigue ductility exponent	c	-0.53

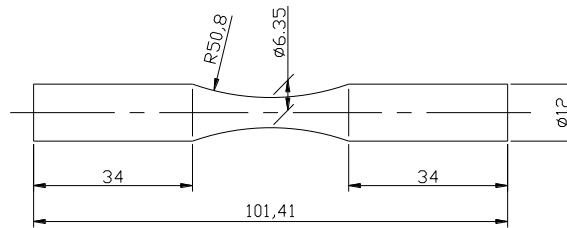


Figure 1. Specimen geometry used in experimental work (dimensions in mm).

All the experimental tests were performed in load control mode in a biaxial servo-hydraulic machine in cyclic tension-compression with cyclic torsion. Test conditions were as follows: frequency 3-5 Hz at room temperature and laboratory air. Tests were interrupted at specimen failure or after 1.5×10^6 cycles.

In order to perform the experimental study different loading paths were defined which are illustrated in Fig. 2, where loading case 0 is a combination of sinusoidal loadings at the same frequency and in phase and case 1 differs from the previous one because there is a lag of 90° between axial and shear loading. Fig. 2a) presents four sequential loading cases, i.e. loading sequences of tension and torsion stresses differing each other by the number of reversals and sequences; Fig. 2b) presents three asynchronous loading cases, where case 6 and 7 result from the combination of loadings with a dual-frequency from each other and in phase and finally, case 8 is obtained with a torsional frequency five times higher than axial stress frequency and in phase. The stress system employed is defined by $\sigma(t) = \sigma \sin(\omega t) + \sigma_0$ and $\tau(t) = \tau \sin(\omega t) + \tau_0$. The

multiaxial fatigue tests were conducted with a constant stress amplitude ratio between axial and torsion of $\sigma = \sqrt{3}\tau$.

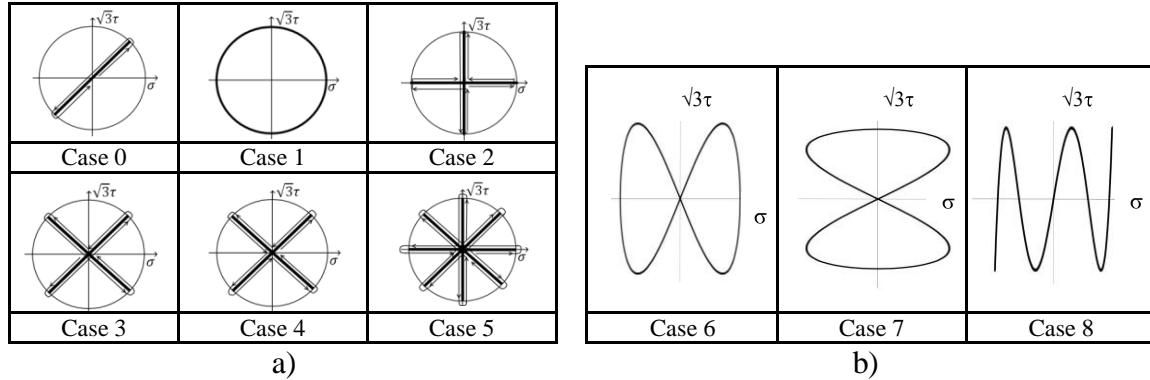


Figure 2. Loading paths carried out: a) Sequential multiaxial loadings; b) Asynchronous multiaxial loadings.

MULTIAXIAL FATIGUE DAMAGE MODELS

From the microscopic scale, the mechanism of crack initiation in ductile metal crystals is the alternating dislocation movements along a slip plane in a grain. This slip is introduced by an alternating shear stress in the slip plane. If the amplitude of the alternating shear stress τ_a exceeds a critical value, a crack will initiate and then will grow out of the grain and becomes a macroscopic crack. Therefore, it is generally assumed that crack initiation in ductile materials is mainly controlled by the amplitude of alternating shear stress τ_a .

An early comprehensive review on multiaxial fatigue was given by Garud [5], the existing multiaxial fatigue models are classified as stress-based, strain-based, energy-based, and fracture mechanics based. Most existing multiaxial fatigue criteria are based on the stress and strain quantities on the macroscopic scale without a direct consideration of the influence of the microscopic features. A recent effort made by McDowell et al. [6] and Xue et al. [7] evaluated the sensitivity of fatigue response to various microstructural features using a multistage model. The more physically-based model was successfully used for an aluminium alloy and a cast alloy to support materials process design and component specific tailoring of fatigue resistant materials.

The critical plane approaches are based on the experimental observations of the early fatigue damage which usually emerges as a micro crack. According to the orientation of a fatigue crack (which always shows some scatter), a corresponding plane can be identified where the fatigue damage accumulation is a maximum among all the possible material planes. The critical plane approaches claim that it is sufficient for the assessment of multiaxial fatigue to consider mechanical quantities as stresses, strains, or both related to the particular planes. The critical plane itself has to be identified in the

course of the assessment by the process of usually maximizing the hypothetical damage parameter with respect to the orientation of the material plane [8].

In contrast to the general trend of applying the critical plane approaches, research also continues on the integral approaches. Within the integral approaches, either all planes are assumed to be involved in the formation of fatigue damage or a scalar quantity without any reference to a material plane orientation is defined as the damage parameter. The shear stress intensity hypothesis [9] is an example for averaging the damage contributions over all planes. The strain energy densities are most often used as the scalar quantities to indicate fatigue damage.

A common feature of many multiaxial fatigue criteria is that they are expressed as a general form and include both shear stress amplitude τ_a and normal stress σ during a loading cycle:

$$\tau_a + k(N_f)\sigma = \lambda(N_f) \quad (1)$$

Multiaxial fatigue models differ in the interpretation of how shear stress amplitude τ_a and normal stress σ in Eq. (10) are defined. For example, the Findley [10], McDiarmid [11] and Dang Van [12] criteria use forms of the range of maximum shear stress, while the Sines [13] and Crossland [14] criteria make use of the octahedral shear stress range. Mean stresses have been incorporated into the models by using either the hydrostatic stress (such as Sines, Crossland and Dang Van, etc.) or the normal stress on a plane (such as McDiarmid, etc.).

Theoretical analysis with critical plane models

For the biaxial loading cases studied in this paper, both the fatigue life and the potential crack plane orientation are analyzed by various critical plane models such as the Findley [10], the Brown-Miller [15, 16], Wang and Brown [17], the Fatemi-Socie [18] and the Smith-Watson-Topper [19]. For structural materials, multiaxial fatigue models gave different damage parameters by introducing the material dependent parameter in the respective damage parameter formulations.

Findley model

Based on physical observations of the orientation of initial fatigue cracks in steel and aluminium, Findley [10] discussed the influence of normal stress acting on the maximum shear stress plane. A critical plane model was introduced, which predicts that the fatigue crack plane is the plane of orientation θ which maximize the Findley damage parameter, Eq. (2):

$$\left(\frac{\Delta\tau}{2} + k\sigma_n \right) = f(\theta) \quad (2)$$

where $\Delta\tau/2$ is the shear stress amplitude on a plane θ , σ_n is the maximum normal stress on that plane and k is a material parameter. For the case of finite long-life fatigue it comes:

$$\left(\frac{\Delta\tau}{2} + k\sigma_n\right) = \tau_f^* (N_f)^b \quad (3)$$

where τ_f^* is computed from the torsional fatigue strength coefficient, τ_f' .

Brown and Miller model

Analogous to the shear and normal stress proposed by Findley, Brown and Miller [15] proposed that both the shear and normal strain on the plane of maximum shear must be considered. Cyclic shear strains will help to nucleate cracks, and the normal strain will assist in their growth. Later, Kandil, Brown and Miller [16] proposed a simplified formulation of the theory for case A cracks. More recently, Wang and Brown [17] added a mean stress term to the formulation, the equivalent shear strain amplitude was formulated as:

$$\frac{\Delta\hat{\gamma}}{2} = \frac{\Delta\gamma_{\max}}{2} + S\Delta\varepsilon_n \quad (4)$$

where $\Delta\hat{\gamma}$ is the equivalent shear strain range and S is a material-dependent parameter that represents the influence of the normal strain on material crack growth and is determined by correlating axial and torsion data, $\Delta\gamma_{\max}$ is taken as the maximum shear strain range and $\Delta\varepsilon_n$ is the normal strain range on the plane experiencing the shear strain range $\Delta\gamma_{\max}$. To compute fatigue life, Eq. (5) can be considered:

$$\frac{\Delta\gamma_{\max}}{2} + S\Delta\varepsilon_n = A\frac{\sigma_f'}{E}(2N_f)^b + B\varepsilon_f'(2N_f)^c \quad (5)$$

where $A=1.3+0.7S$, and $B=1.5+0.5S$.

Fatemi-Socie model

The Fatemi-Socie (F-S) model [18] is widely applied for shear damage model, which predicts that the critical plane is the plane of orientation θ with the maximum F-S damage parameter:

$$\frac{\Delta\gamma}{2} \left(1 + k \frac{\sigma_{n,\max}}{\sigma_y}\right) = f(\theta) \quad (6)$$

where $\Delta\gamma/2$ is the maximum shear strain amplitude on a plane θ , $\sigma_{n,\max}$ is the maximum normal stress on that plane, σ_y is the material monotonic yield strength; k is a material constant, which can be found by fitting fatigue data from simple uniaxial tests to fatigue data from simple torsion tests, $k=1.0$ for 42CrMo4.

$$\frac{\Delta\gamma}{2} \left(1 + k \frac{\sigma_{n,\max}}{\sigma_y} \right) = \frac{\tau_f'}{G} (2N_f)^{b_\gamma} + \gamma_f' (2N_f)^{c_\gamma} \quad (7)$$

where G is the shear modulus, τ_f' is the shear fatigue strength coefficient, γ_f' is the shear fatigue ductility coefficient, and b_γ and c_γ are shear fatigue strength and shear fatigue ductility exponents, respectively.

Smith-Watson-Topper model

The S-W-T tensile damage model, proposed by Smith, Watson and Topper [19], predicts that the fatigue crack plane is the plane of orientation θ with maximum normal stress (the maximum principal stress):

$$\sigma_{n,\max} \frac{\Delta\varepsilon_1}{2} = f(\theta) \quad (8)$$

where $\Delta\varepsilon_1/2$ is the maximum principal normal strain amplitude and $\sigma_{n,\max}$ is the maximum normal stress on the $\Delta\varepsilon_1$ plane.

To compute fatigue life Eq. (9) was considered:

$$\sigma_{n,\max} \frac{\Delta\varepsilon_1}{2} = \frac{\sigma_f'^2}{E} (2N_f)^{2b} + \varepsilon_f' \sigma_f' (2N_f)^{b+c} \quad (9)$$

For each loading case and for each model the critical plane angle θ was identified and achieved. Some results are presented and discussed in the next section.

RESULTS AND DISCUSSION

Fatigue Life Results

Figs 3 and 4 present the results of the fatigue life obtained using von Mises criterion for calculating the equivalent multiaxial stress for the various loading paths carried out on this study, with the sequential and asynchronous effects, respectively.

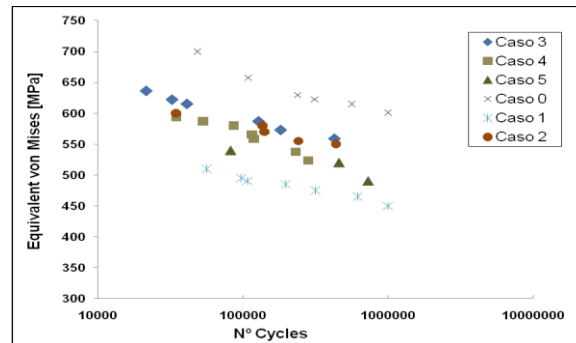


Figure 3. Results of the fatigue life for the sequential loading paths.

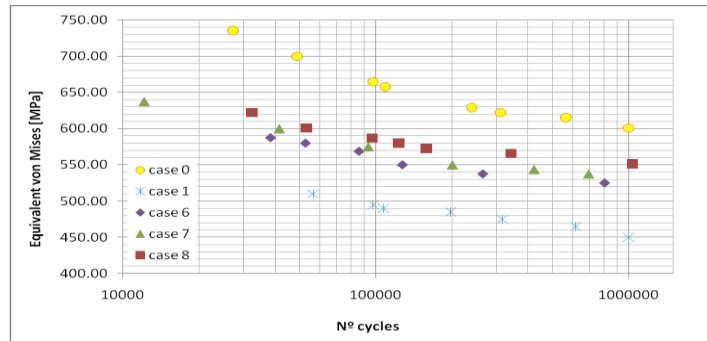


Figure 4. Results of the fatigue life for the asynchronous loading paths.

Concerning Figs. 3 and 4, the cases taken as reference, cases 0 and 1, respectively, are those that cause extreme (minor and major) damages to the material. All the remaining cases, either sequential or asynchronous loading cases lead to less damage than non-proportional loading (case 1) to the material but causes greater damage than proportional loading. The presence of multiple torsion cycles at higher frequency in asynchronous loading paths does not mean an increased damage accumulation when compared with non proportional loading cases.

Cyclic Plasticity Model

Numerical simulations were conducted by application of the advanced cyclic plasticity model of Jiang and Sehitoglu [4]. Since the experiments were carried out in load control in the present research, the cyclic strains were calculated using the cyclic stresses as input to the model.

Jiang and Sehitoglu's plasticity model [4] uses the Mises yield function, the normality flow rule, a hardening rule and material memory. There are four material parameters in Jiang model, c , r , x , and k that must be determined. All of these constants are computed from the cyclic stress strain curve of the material. The shear yield strength, k , is obtained by setting the plastic strain to 0.002 (0.2%) and dividing by $\sqrt{3}$. Both c and r are obtained by selecting a series of stress strain pairs along the material cyclic stress strain curve and describe the shape of the curve. Ratcheting rate is controlled by x which is set at a fixed value of 5.

Simulated Stress/Strain Results

All the loading paths used on experimental testing were simulated using the Jiang cyclic plasticity model. As an example, in Figs 5, 6, and 7 are shown the simulation results of the stress loading path used on testing, and the evolution of the shear strain and axial strain (strain path), for some selected loading paths in order to compare the estimations of the models and the experimental values of fatigue life.

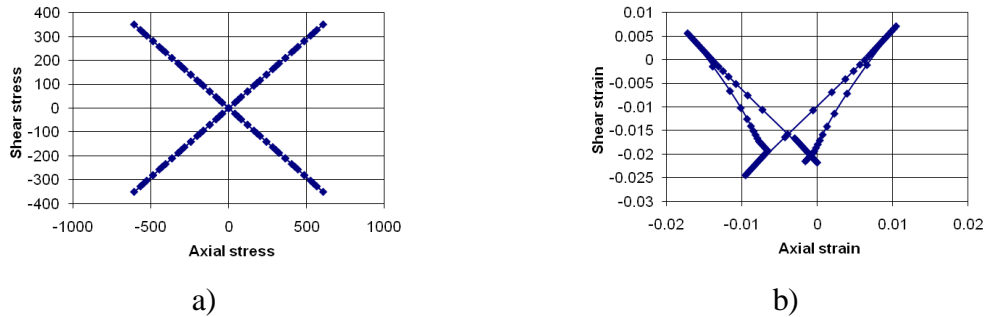


Figure 5. Simulation results from the sequential loading case 3: a) Stress control; b) Strain path result.

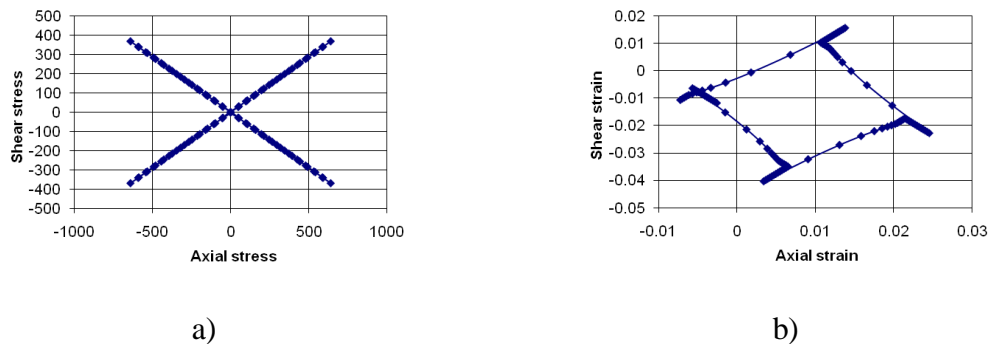


Figure 6. Simulation results from the sequential loading case 4: a) Stress control; b) Strain path result.

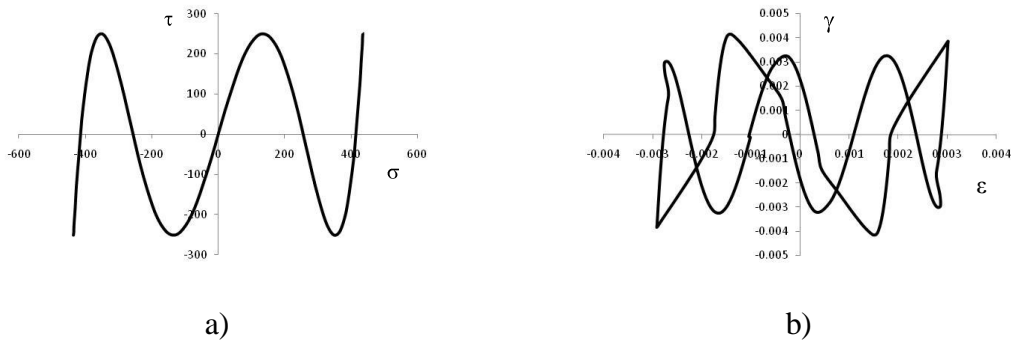


Figure 7. Simulation results from the asynchronous loading case 8: a) Stress control; b) Strain path result.

In Fig. 8 it is presented, also as an example, comparisons between the fatigue life estimations, considering the Fatemi –Socie model, and the experimental values of fatigue life for the asynchronous loading case 8. In Fig. 8b) the comparison is made taking into account the Jiang and Sehitoglu cyclic plasticity model.

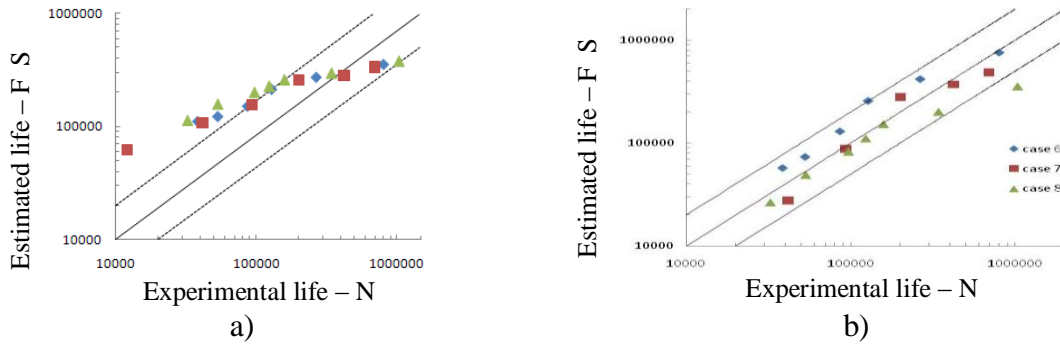


Figure 8. Comparison between experimental and estimated fatigue life: a) without and (b) with the application of the cyclic plasticity model for the damage parameter F-S, asynchronous loading cases 6 to 8.

Analysing the data on Fig. 8 it is possible to observe the influence of the cyclic plasticity model results when fatigue lives are compared. Life estimations below 10^5 cycles are quite improved by the model output, contributing to a better accuracy of the results.

Damage Accumulation Analysis

The angles of the critical plane of crack initiation were obtained experimentally with the help of optical and scanning electron microscopy (SEM), as shown in Fig. 9 a) and had been compared with the theoretical results using the critical plane models of Findley, Brown-Miller, SWT and Fatemi-Socie. The 3D approach of damage surface allows to get more information than that would be gotten using only the method 2D, [20]. Fig. 9b) shows, as an example, the 3D surface of damage for loading case 5 using the Brown-Miller model, where multi-damage planes are activated, [21].

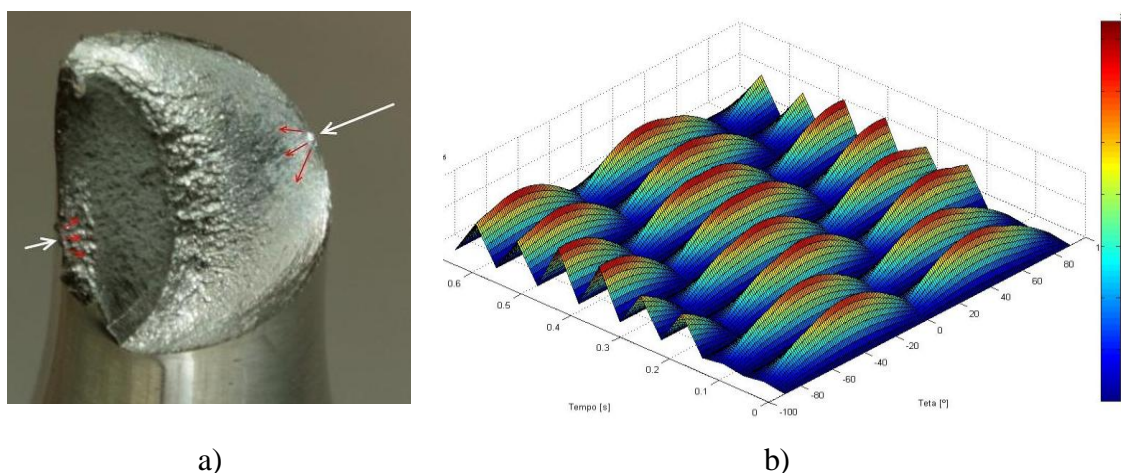


Figure 9. a) Fractographic analysis of fracture surface under sequential loading case 4; b) Brown and Miller evolution parameter in sequential loading path, case 5.

The shear strain evolution in the critical plane during a cycle of loading path, allows determining the damage accumulation of each loading path. This damage is important for the cases of asynchronous loading paths where the determination of the number of cycles may allow several interpretations. As an example, and taking the shear strain values from the critical plane in function of time for one cycle of loading path, it can be plotted Fig. 10, where it is easy to identify the various existing cycles, i.e., four small cycles with an intensity one order of magnitude below the main cycle. As such, the expected life for the four small cycles is much higher than the infinite life level being above 10^{12} cycles for all methods of predicting the fatigue life, thereby, causing irrelevant material damage. Thus, it can be concluded that, in the cases under study, it is a good approximation to consider only a single cycle for each loading path conclusion.

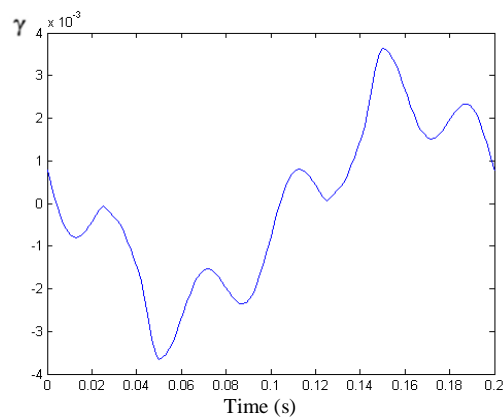


Figure 10. Shear strain evolution in asynchronous loading case 8.

CONCLUSIONS

The effects of sequential and asynchronous loading paths on damage accumulation and consequently in fatigue life is studied and discussed in this paper. Various multiaxial loading paths, regarding the structural steel -42CrMo4- were both experimental and computational carried out. Based on this study some conclusions can be drawn:

- Cyclic stress/strain states are influenced by the multiaxial loading paths, i.e. the sequential loading and the asynchronous effects are determinant factors in damage accumulation and consequently in fatigue life.
- Critical plane criteria used in this study produced reasonable estimates of crack initiation angles by comparison with the experimental results.
- For a correct fatigue life estimation the use of adequate cyclic plasticity models to predict the actual strain values is essential.
- For the axial-shear relation studied, sub cycles present in the various loading path do not show relevant magnitude to cause relevant damage.
- In the present study, loading control was applied due to the consideration that plain stress state generally occurs on the surface of components. Therefore, it would be helpful to understanding the stress-strain evolutions under the stress control conditions.

ACKNOWLEDGEMENTS

The work was financed by FCT – Fundação para a Ciência e a Tecnologia, Portuguese Science Foundation through the Project PTDC/EME-PME/104404/2008. The authors are grateful to Prof. D. Socie of UIUC for providing software of implementation of the Jiang and Sehitoglu's plasticity model.

REFERENCES

1. Fatemi, A and Yang, L. (1998) *Int. J. Fatigue* **20**(1), 9–34.
2. Weiss, J and Pineau, A. (1993) In: *Advances in Multiaxial Fatigue*, ASTM STP **1191**, 183–203, D.L. McDowell and R. Ellis (Eds.).
3. Ott, W., Chu, C.-C., Trautmann, K.-H., Nowack, H., (2000) In: *Ellyn, F., Provan, W. (Eds.), Proc. 8th Int. Conf. Mech. Behaviour Mat. (ICM 8)*, pp. 1204–1209.
4. Jiang, Y., Sehitoglu, H. (1996) *ASME J. Appl. Mech.* **63**, 720–725.
5. Garud, Y.S. (1981) *J. Test. Eval.* **9**, 165–178.
6. McDowell, D.L., Gall, K., Horstemeyer, M.F., Fan, J. (2003) *Eng. Fract. Mech.* **70**, 49–80.
7. Xue, X., McDowell, D.L., Horstemeyer, M.F., Dale, M.H., Jordon, J.B. (2007) *Eng. Fract. Mech.* **74**, 2810–2823.
8. Jiang Y., Ott W., Baum C., Vormwald M., Nowack H. (2009) *International Journal of Plasticity* **25**, 780–801.
9. Zenner, H., Simbürger, A., Liu, J. (2000) *Int. J. Fatigue* **22**, 137–145.
10. Findley WN (1959) *Journal of Engineering for Industry*, 301-306.
11. McDiarmid DL (1991) *Fatigue Fract. Eng. Mater. Struct.* **14**, 429–453.
12. Dang-Van K. (1993) In: *Advances in Multiaxial Fatigue*, ASTM STP 1191. eds. D. L. McDowell and R. Ellis, ASTM, Philadelphia, 120-130.
13. Sines G. (1959) In: *Metal Fatigue*, G. Sines and J.L. Waisman. Eds., McGraw Hill, 145-169.
14. Crossland, B. (1956) *Proc. Int. Conf. on Fatigue of Metals*.
15. Brown, M. W. and Miller, K. J. (1973) Proceedings of the institute of mechanical engineers, Vol. 187, pp. 745-756.
16. Kandil, F. A., Brown M. W. and Miller, K.J. (1982) the Metals Society, London, pp.203-210.
17. Wang, C. H. and M. W. Brown (1996) *Journal of Engineering Materials and Technology-Transactions of the ASME* **118**(3): 367-370.
18. Fatemi, A. and Socie, D. (1988) *Fatigue and Fracture of Engineering Materials and Structures*, **11**(3), 149-165.
19. Smith, R.N., Watson, P. and Topper, T.H. (1970) *J. of Materials* **5**(4), 767-778.
20. Reis, L., Li, B. and Freitas, M. de (2006). *Fracture of Engineering Materials and Structures*, Vol. 29 (4), pp.281-289.
21. L. Reis, L., Anes, V., Li, B. and Freitas, M. de. *Proc. 2^a Int. Conf. on Material and Component Performance under Variable Amplitude Loading*, 23 - 26 March, Darmstadt, Germany, 2009.